Proceedings of the SPATIAL SCIENCES & SURVEYING BIENNIAL CONFERENCE 2011
21-25 November 2011, Wellington, New Zealand

Disaster Change Detection Using Airborne LiDAR

John Trinder
School of Surveying and Spatial Information Systems, The University of New South Wales
UNSW SYDNEY NSW 2052, Australia
j.trinder@unsw.edu.au

Mahmoud Salah
Dept. of Surveying, Faculty of Engineering Shoubra, Benha University
108Shoubra Street, Cairo, Egypt
engmod2000@yahoo.com

ABSTRACT

Potential applications of airborne LiDAR for disaster monitoring include flood prediction and assessment, monitoring of the growth of volcanoes and assistance in the prediction of eruption, assessment of crustal elevation changes due to earthquakes, and monitoring of structural damage after earthquakes. Change detection in buildings is an important task in the context of disaster monitoring, especially after earthquakes. The paper will describe the capability of airborne LiDAR for rapid change detection in elevations, and methods of assessment of damage in made-made structures. The approach is to combine change detection techniques such as image differencing, principal components analysis (PCA), minimum noise fraction (MNF) and post-classification comparison based on support vector machines (SVM), each of which will perform differently, based on simple majority vote. In order to detect and evaluate changes in buildings, LiDAR-derived DEMsfrom two epochs were used, showing changes in urban buildings due to construction and demolition. To meet the objectives, the detected changes were compared against reference data that was generated manually. The comparison is based on three criteria: overall accuracy; commission and omission errors; and completeness and correctness.The results showed that the average detection accuracies were: 84.7%, 88.3%, 90.2% and 91.6% for post-classification, image differencing, PCA and MNF respectively. On the other hand, the commission and omission errors, and completeness and the correctness of the results improved when the techniques were combined,compared to the best single change detection method. The proposed combination of techniques gives a high accuracy of 97.2% for detection of changes in buildings, which demonstrates the capabilities of LiDAR data to detect changes, thus providing a valuable tool for efficient disaster monitoring and effective management and conservation.

KEYWORDS: LiDAR, Change detection, Building extraction, Feature extraction.

1 INTRODUCTION AND RELATED WORKS

An up-to-date building database is a crucial requirement for reliable disaster damage assessment. Change detection employing LiDAR(Light Detection and Ranging)data is a useful tool for damage detection, particularly for collapsed multi-floored buildings (Tuong et al., 2004). LiDARsare active acquisition systems equipped with a laser scanner, a Global Positioning System (GPS) receiver and an Inertial Navigation System (INS). They emit infrared laser pulses at high frequency and record the time of flightof the return pulses.By combining the LiDAR distance with GPS and INS data the X, Y and Z coordinates of ground points can be determined. The intensity of the returns can also be recorded. There are basically two types of LiDAR systems: discrete and waveform. A short pulse (~ns) is emitted from the laser and in discrete systems one or more

discrete distances and intensities are recorded. Waveform systems record the full waveform of the return signal.

Methods of change detection can mainly be divided into two categories:

- The determination of the difference of classifications of a surface obtained at two periods;
- The direct determination of change between two data sets.

Detecting changes by supervised classification is unreliable when the appearances of non-buildings and buildings are similar. Furthermore, using spectral information to detect change does not consider the situation when the differences occur in shape instead of colour (Huang and Chen, 2007). A number of research results, such as Knudsen and Olsen (2003), Matikainen et al. (2004), Walter (2004a, b) and Nielsen and Canty (2011) belong to the first category above. The second category [Murakami et al., 1999; Jung, 2004] is unable to determine the land category because no classification is used. It is also observed that trees often cause mistakes in the output of research.

Even though aerial photography has been conventionally employed for change detection [Niederöst, 2001; Knudsen and Olsen, 2003; Walter, 2004a; Walter, 2004b], aerial photographyis subject to several unavoidable problems such as: shadows in the scenes acquired over dense urban areas with many skyscrapers; the spectral information of certain features in aerial photography is diverse and ill-defined (Knudsen and Olsen, 2003); perspective projection causes relief displacement of buildings, which requires height information to correct. Therefore, the employment of LiDARdata rather than spectral information derived from aerial photographs offers important advantages (Tuong, et al., 2004). It allows obtaining 3D point clouds of the surface with high density as well as high accuracy. Moreover, the method is capable of collecting data over large areas in a short time (Baltsavias, 1999).

Instead of the multi-spectral imagery that was often used in the past, many change detection methods using LiDAR data have been proposed. Murakami et al., (1999) carried out change detection of buildings using LiDAR data in Japan. That study was a simple comparison between two datasets. Tuong et al., (2004) presented an automatic method for LiDAR-based change detection of buildings in dense urban areas. Walter (2004b) used LiDAR data in an object-based classification to determine the land-use category after the observation of land phenomena. Matikainen et al. (2004) divided a LiDAR point cloud into homogeneous areas, and then extracted information to discover the building areas for change detection. Girardeau-Montau et al. (2005) directly used point-to-point position relations for change detection. Huang and Chen (2007)included LiDAR data and aerial images to detect the changes of building models. Brzank et al., (2009) presented a new method to detect and evaluate morphologic changes of the Wadden Sea based on the extraction of structure lines of tidal channels from LiDAR data. Chien and Lin (2010) developed a new methodto find changes within 3D building models in the region of interest with the aid of LiDAR data. Their modelling scheme comprises three steps, namely, data pre-processing, change detection in building areas, and validation. Research findings clearly indicate that the double-threshold strategy improves the overall accuracy from 93.1% to 95.9%.

It is worth mentioning that, as change detection is an important step in data updating, some methods used spectral-based methods such as the iterative principal components analysis (IPCA) to determine temporal distance in feature space and combine it with a Bayesian decision rule to determine the presence of change (Spitzer ***et al.***, 2001). Clifton (2003) describes training neural networks to learn expected changes between images and to then identify pixel changes which do not match what is “expected”. Hashimoto et al. (2011) proposed a knowledge-based change detectionapproach, which can obtain change information thatincludes not only land cover changes, but also contextualchanges, such as types of damage caused by natural hazards.This approach mainly consists of two processes: informationextraction and change inference using a Bayesian network.Information extraction employs object-based image analysisfor extracting spatial information. Change inference usesextracted information and the Bayesian networkconstructed from knowledge of the change detection process. Todemonstrate this approach, change detection of mudslidedamage caused by heavy rain in Yamaguchi Pref., Japanwas conducted.Some other methods used multi-temporal high-resolution imagery to detect changes in spectral difference or used supervised classification to determine building positionsfor comparisons of two epochs for change detection (Knudsen and Olsen, 2003; Kumar, 2011).

This paper describes a proposed workflow for LiDAR-based change detection. The paper is organised as follows. Section 2 describes the study areas and data sources. Section 3 describes

the experiments while Section 4 presents and evaluates the results. We summarise our results in Section 5.

2 STUDY AREAS AND DATA SOURCES

2.1 LiDAR data

No data was available before and after an earthquake, but in order to demonstrate the capability of the proposed change detection method, two LiDAR data sets were available,acquired on different occasionsover Tokyo, which is an earthquake-prone area in Japan. Survey flights were carried out by Asia Air Survey Co. Ltd in June 1999 and February 2004. The sensor and scene characteristics of the used data are summarized in Table 1. Data was provided in 1m^2 grid formats over a dense urban area which includes residential buildings, large buildings, a network of main and local roads, open and green areas as well as trees. The pulse intensity is recorded in more recentLiDAR systems but it has not been a concern in this study.Figure 1 shows the acquired LiDAR data in grid format.It is worth mentioning that the test areas have been used in previous studies (Tuong et al., 2004) for change detection, which used a simple method to form the difference image based on a histogram thresholding and different reference data. The results showed 55% error in detecting new demolitions.

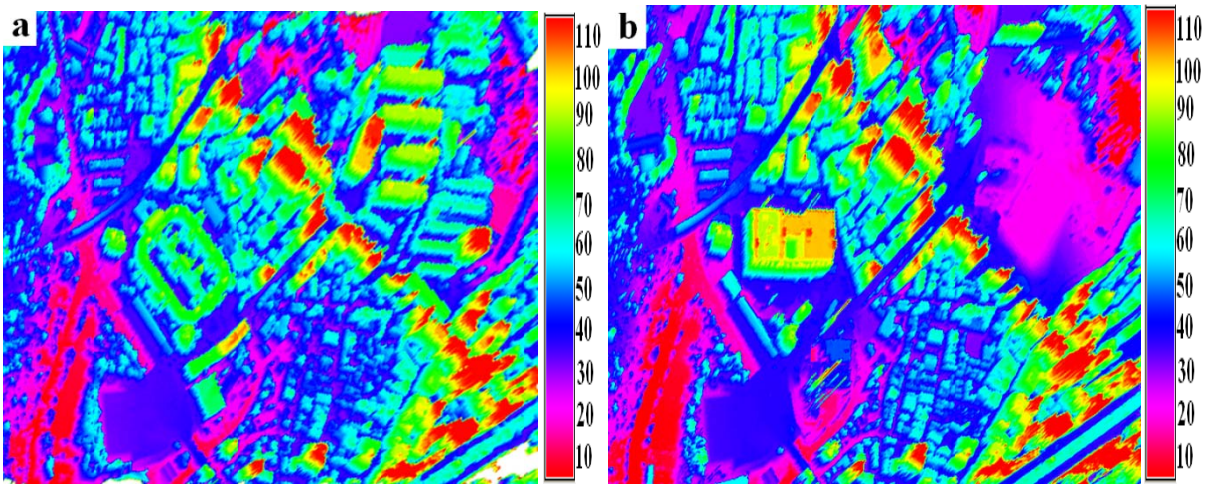

Figure 1: Acquired LiDAR data in grid format a) June 1999, and b) February 2004.

Table 1: Characteristics of LiDAR datasets.

	First Dataset	Second Dataset
Spacing across track (m)	0.15	0.85
Spacing along track (m)	1.5	1.48
Vertical accuracy (m)	0.15	0.10
Horizontal accuracy (m)	0.5	0.5
Density (Points/m^2)	4	2.5
Sampling intensity (mHz)	125	150
Wavelength (µm)	1.56	1.064
Average altitude (m)	800	1450
Laser swath width (m)	750	777.5
Acquisition date	June 1999	February 2004

2.2 Reference data

In order to accurately evaluate the performance of the proposed change detection method, changes were visually interpreted and digitized independently of their size. The reference data is a

four-class thematic image, typically divided into the four categories of: '*background*'; '*decreased*', '*increased*'; and '*unchanged*' as shown in figure 2.

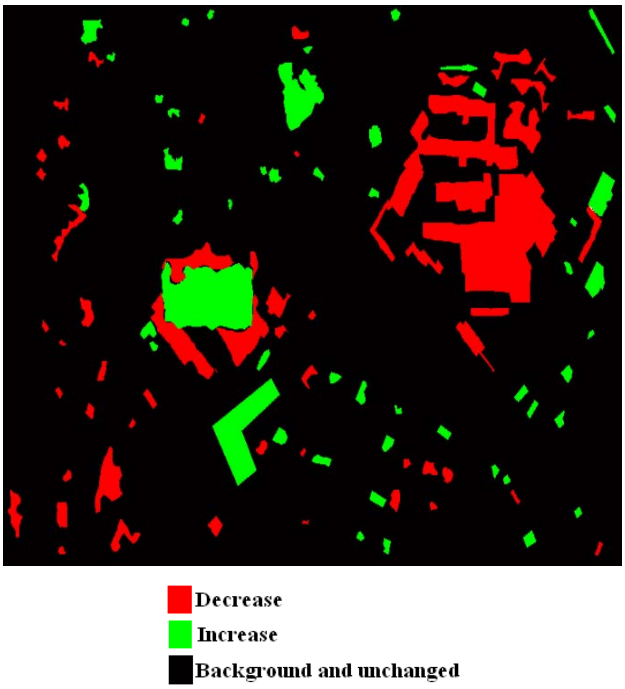

Figure 2: Manually digitized reference changes.

3 METHODOLOGY

3.1 Pre-processing

First, both DEMs were registered to each other based on a projective transformation. The registration process resulted in small Root Mean Square Errors (RMSE) that did not exceed 0.15m in both X and Y directions. Following the transformation, the images were resampled to 1m pixel size. A grid format is preferred tothe raw point cloud formatto speed up the processing, particularly when there is a direct comparison of the two datasets.In order to obtain a high image quality and to reduce the processing time, a bilinear interpolation was applied for the resampling process. The bilinear interpolation can result in a better quality image than nearest neighbourhood resampling and requires less processing than cubic convolution.

3.2 Main-processing

Four different change analyses were performed to evaluate the efficacy of LiDAR data for detecting changes occurring at two different temporal scales. The four methods include: image differencing; principal components analysis (PCA);minimum noise fraction (MNF); and Post-Classification based on support vector machine (SVM). After these steps, a simple majority vote has been applied to generate the change detection image. All the methods proposed in this research were implemented through programs generated by the authors in a Matlab environment. An interface was developed to enable the user to: detect changes through the aforementioned four methods; combine votes derived from all methods; generate a change detection image; and evaluate the change detection results. The workflow for this investigation is shown in figure 3.

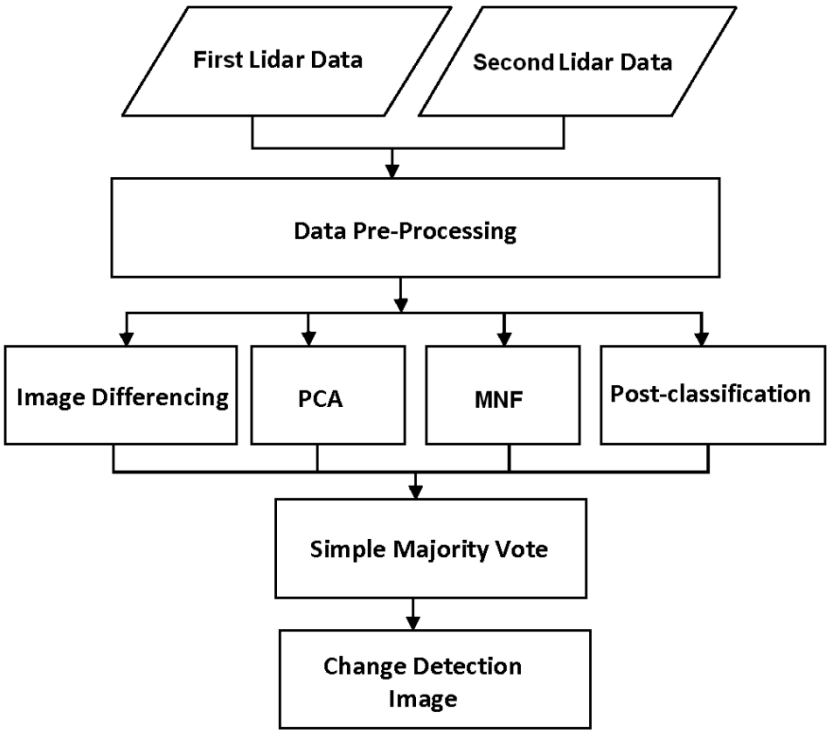

Figure 3: The workflow for the proposed change detection method.

In the first change detection technique, differences between the two DEM images that exceed a user-specified threshold of 10 pixels in area and 0.30m in height, double of the LiDAR system accuracy, were computed and highlighted. In the image differencing method, the second image is subtracted from the first image to provide the difference and highlight changes. The second image is more recent and the differencesreflect changes over time. After application of image differencing, increases in height values that are more than the predefined thresholds, are highlighted as *increases*, while decreases in height values that are more than the predefined thresholds, are highlighted as *decreases*. The result is a grey scale image composed of a single band of continuous data that reflects the changes. The change image is a four-class thematic image, typically divided into the four categories of: *background*; *decreased*, *increased*; and *unchanged*. Although the calculation is simple, the interpretation requires knowledge about the area, because every difference relates to a certain location but not necessarily to the same object.

In the second change detection technique, principal components analysis (PCA) has been applied to detect changes. Principal components analysis (PCA) is commonly applied for orthogonal data transformations. PCA maximizes the spectral variability detected by decreasing the redundancy of information contained in multiple spectral bands (Armenakis et al., 2003). PCA components are based on statistical relationships that are difficult to interpret, and are variable between different landscapes and different dates for a single landscape (Collins and Woodcock 1994). PCA is a linear transformation of the data along perpendicular axes of maximum variance between data sets (Legendre and Legendre 1998). The first eigenvector sorts pixels along an axis of highest correlation between data sets. Pixels on this axis have not significantly changed between the two images. The second eigenvector is perpendicular to the first, and therefore sorts pixels that represent differences between data sets.

In the third change detection technique, the minimum noise fraction Transform (MNF) as modified from Green et al. (1988) has been performed to detect changes. MNF is a linear transformation that consists of the following separate principal components analysis rotations: (i) The first rotation uses the principal components of the noise covariance matrix to decorrelate and rescale the noise in the data (a process known as noise whitening), resulting in transformed data in which the noise has unit variance and no band-to-band correlations; (ii) The second rotation uses the principal components derived from the original image data after they have been noise-whitened by the first rotation and rescaled by the noise standard deviation. The inherent dimensionality of the data is determined by examining the final eigenvalues and the associated images. For the best

results, and to save disk space, only those bands with high eigenvalues have been output. Images with eigenvalues close to 1 are mostly noise.

In the fourth change detection technique, post-classification comparison wasperformed in order to detect changes. The two DEM images were classified using asupport vector machine classifier (SVM), then the classification results were compared and the differences were extracted. The objective is to classify the input data into four primary classes of interest, namely buildings, trees, roads, and ground. SVMs are based on the principles of statistical learning theory (Vapnik, 1979) and delineate two classes by fitting an optimal separating hyperplane (OSH) to those training samples that describe the edges of the class distribution. As a consequence they generalize well and often outperform other algorithms in terms of classification accuracies. Furthermore, the misclassification errors are minimized by maximizing the margin between the data points and the decision boundary.Since the One-Against-One (1A1) technique usually results in a larger number of binary SVMs and then in subsequently intensive computations, the One-Against-All (1AA) technique was used to solve for the binary classification problem that exists with the SVMs and to handle the multi-class problems. The Gaussian radial basis function (RBF) kernel has been used, since it has proved to be effective with reasonable processing times in remote sensing applications.

Then, a simple majority vote, which can be more effective than more complex voting strategies (Waske, 2007), is used to generate the final result. If change detection algorithm $c_i$assigns a given pixel to class label ω_j, then we say that a vote is given to ω_i. After counting the votes given to each class label by all detection algorithms, the class label that receives the highest number of votes is taken as the final output. It is worth mentioning that all votes are of equal weight and independent of height differences.When the four detection methods give completely different decision for a given pixel, which does not convey any information, the decision from the method with highest overall detection accuracy is considered.

As a last step, the smaller detected regions were merged into larger neighbouring homogeneous ones or deleted according to an arbitrary 1m distance and 30m^2 area thresholds respectively. The area threshold represents the expected minimum change area, while the distance threshold was set to 1m to fill in any gaps within the detected region. Regions were retained if they were larger than the given area threshold and/or were adjacent to a larger homogeneous region by a distance less than 1m. Finally, region borders were cleaned by removing structures that were smaller than 5 pixels and that were connected to the region border. There was a compromise between cleaning thresholds less than 5 pixels, which may leave the original buildings uncleaned, and thresholds greater than 5 pixels which may remove parts of the detected region. The result was an image that represents the detected changes without noisy features and also without holes.

3.3 Evaluation of the change detection results

In order to evaluate the performance of the adopted method for change detection from LiDAR data, the results have been checked based on three different methods which include: (i) The overall detection accuracy; (ii) The produced omission and commission errors; and (iii) The completeness and correctness of the results.

The overall accuracy for the detection process was assessed using the reference data and based on equation 1:

$$ODA = \frac{NCP}{NRP} \tag{1}$$

Where *ODA* is the overall detection accuracy; *NCP*is the total number of correctly detected pixels and *NRP* is the total number of reference pixels.

Since the overall detection accuracy is a global measure for the performance of the combination process, two additional measures were used to evaluate the performance of the proposed combination method, namely: commission and omission errors(Congalton, 1991). Unlike overall detection accuracy, commission and omission errors clearly show how the performance of the proposed methods improves the results or cause a deterioration of resultsfor each individual class compared to the reference data.

$$CE_I = \frac{A_1 + A_2 + A_3}{R_1} \quad (2)$$

$$OE_I = \frac{B_1 + B_2 + B_3}{R_1} \quad (3)$$

CE_I and OE_I are commission and omission errors of class *increased*; A_1, A_2 *and* $A_3$are the numbers of incorrectly identified pixels of class *increased* associated with classes *decreased*, *background* and *unchanged*; R_1 is the total number of pixels of the class *increased* as observed in the reference data; B_1, B_2 *and* B_3 are the numbers of unrecognized pixels that should have identified as belonging to the class *increased*. The same is applicable for classes *decreased*.

On the other hand, in order to evaluate the performance of the change detection process, the *completeness* and the *correctness*(Heipke et al., 1997) of the detected changes were investigated based on a per-pixel as follow:

$$Completeness = \frac{TP}{TP + FN} \quad (4)$$

$$Correctness = \frac{TP}{TP + FP} \quad (5)$$

TP denotes to the number of true positives which is the number of entities that were automatically detected and were available in the reference data. *FN* relates to the number of false negatives which is the number of entities that were available in the reference data but not automatically detected. *FP* stands for the number of false positives which is the number of entities that were automatically detected but do not correspond to any entities in the reference data (Rottensteineret al., 2007).

4 RESULTS AND ANALYSIS

Figure 4 is a typical example showing the results in a sub-area of the whole test area. For the detected changes, the green colour indicates an *increase*, the red colour labels a *decrease* while black colour refers to both *background* and *unchanged*. It can clearly be seen that the important changes occur in buildings. In the middle of the area the large building has been replaced with a new one with a different shape. At the lower right part of the area, some new buildings have been constructed.

Another aspect of interest is where the misclassified pixels were recovered by the combination process. Most corrections occur at the edges of buildings and trees, which demonstrates the effect of between-class variance on the edge pixels which caused many of these pixels to be placed in an incorrect category. It can clearly be seen that the detected changes for PCA are eroded as compared to the reference data. This trend can also be observed for post-classification results. On the other hand, the detected changes for image differencing are larger. However, the erosion effect has been reduced after applying the MNF and the simple majority vote combination.

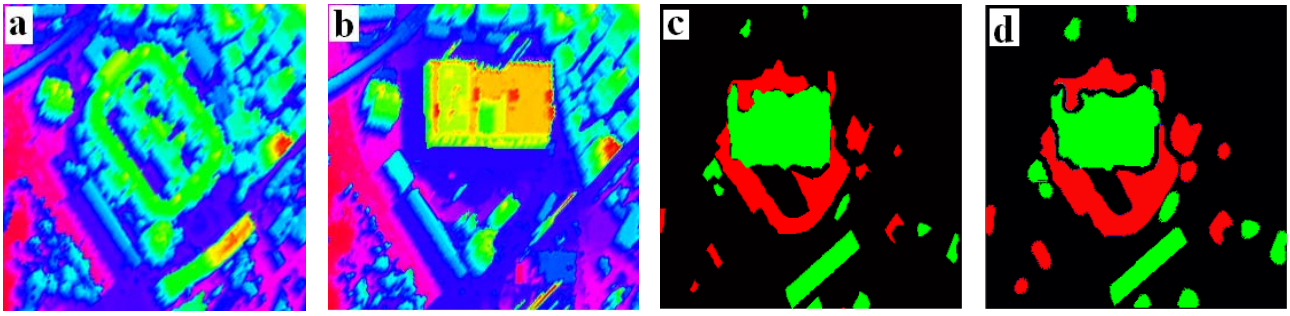

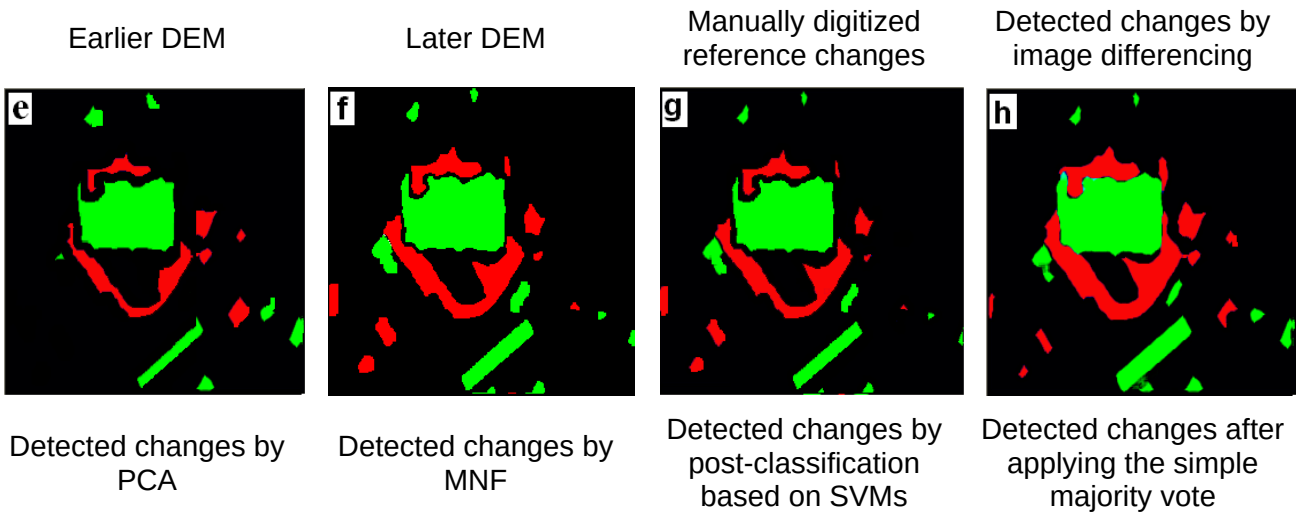

Figure 4: Typical example of the change detection results. Areas in red are classified as *decreased*; areas in green are classified as *increased*; while areas in black refer to both *background* and *unchanged*.

The overall detection accuracies of individual techniques, based on the reference data, are given in Table 2. MNF performed the best with 91.6% detection accuracy, followed by PCA, image differencing and post-classification with detection accuracies of 90.2%, 88.3% and 84.7% respectively.

The improvement in detection accuracies achieved by the combination method compared with the best individual detection technique, MNF, was determined as shown in Table2. It is clear that the performances of simple majority voteare better than those of single detection methods. The improvement in detection accuracy of 5.6% is obtained from simple majority votealgorithm.

Table 2: Performance evaluation of single detection techniques.

Method	**Detection accuracy (%)**
image differencing	88.3
PCA	90.2
MNF	91.6
post-classification	84.7
simple majority vote	97.2

Table 3 shows the commission and omission errors based on the proposed method, compared to the commission and omission errors of the best individual methods. It can be seen that a considerable amount of the misclassified pixels have been recovered by the combination process. For the best change detection method, MNF, the omission errors vary from 8.08% to 10.65%, while the commission errors range from 6.17% to 9.28% respectively. For the combined change detection method based on the simple majority votealgorithm, the omission errors range from 2.87% to 7.03%, while the commission errors range from 3.32% to 6.11% respectively.The most important point to note is that both types of errors using simple majority vote are comparable. This indicates the capabilities of the proposed method to detect changes from LiDAR data. Figure 5, which is a typical example of the error distribution map, showing that omission and commission errors mostly occurred at the building outlines.

It is worth mentioning that some differences along the edges of buildings are not real changes. One possible reason for these differences is the random reflectance of laser pulses. Another possible reason could be the differences between parameters of the two surveying flights. The flight in 1999 was collected in summer while the flight in 2004 was collected in winter; many of detected ‘demolitions’ were trees. It can be concluded that trees are the main cause of commission

errors. There seems to be no mechanism to check the omission errors, which supports previously reported findings (Tuong et al., 2004).

Table 3: Change detection errors of the proposed method compared with those of the individual methods. Com. and Om. Stand for commission and omission errors respectively.

	post-classification		**image differencing**		**PCA**		**MNF**		**simple majority vote**	
	Om. (%)	**Com. (%)**	**Om. (%)**	**Com. (%)**	**Om. (%)**	**Com. (%)**	**Om. (%)**	**Com. (%)**	**Om. (%)**	**Com. (%)**
Increased	19.02	11.93	11.68	9.38	10.30	09.31	8.08	09.28	02.87	03.32
Decreased	21.50	11.98	16.89	11.46	13.09	07.32	10.65	06.17	07.03	06.11

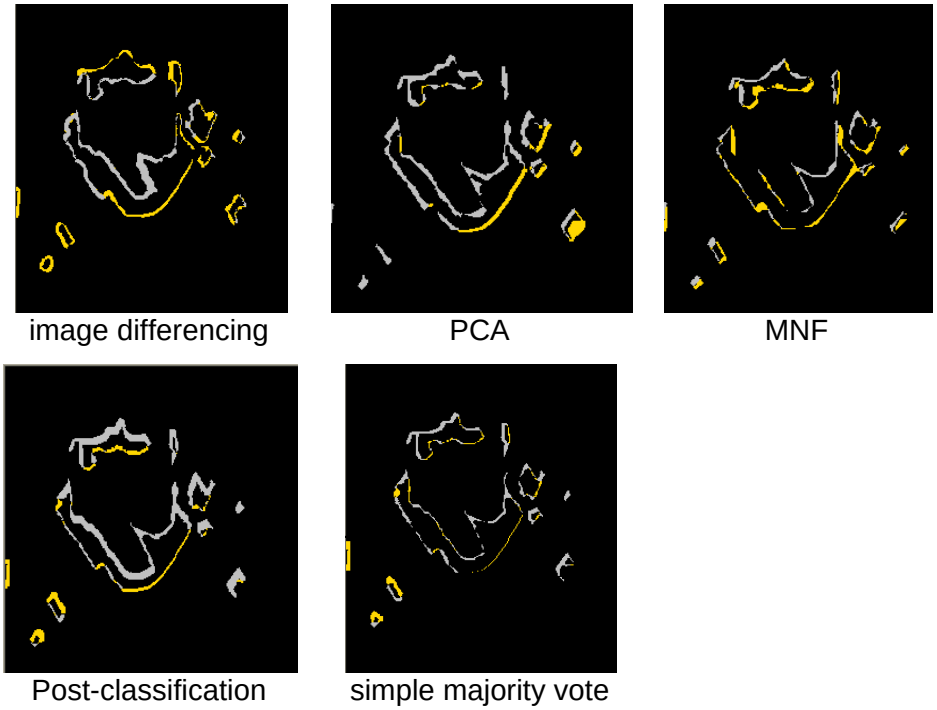

Figure5: Evaluation of the results of change detection. Black: correct changesin pixels; grey: omission errors; yellow: commission errors.

For the per-region based evaluation, a region was counted as a true positive if at least 90% of its area from the automatically detected results was overlapped by the corresponding area in the reference data. Figure 5 shows the completeness and correctness against the region size. The completeness and correctness of regions around 30m^2 were around 79% and 75% respectively and these statistics improve as the region size increased. Completeness and correctness were over 91% for all regions larger than 50m^2. The difference between completeness and correctness is a matter of 0.1–1% except for regions smaller than 50m^2 where the difference is up to 4%. This further confirms the lower reliability of detecting regions smaller than 50m^2. It can therefore be concluded that these tests strongly represent achievable accuracies for detection of changes by the proposed method using LiDAR data.

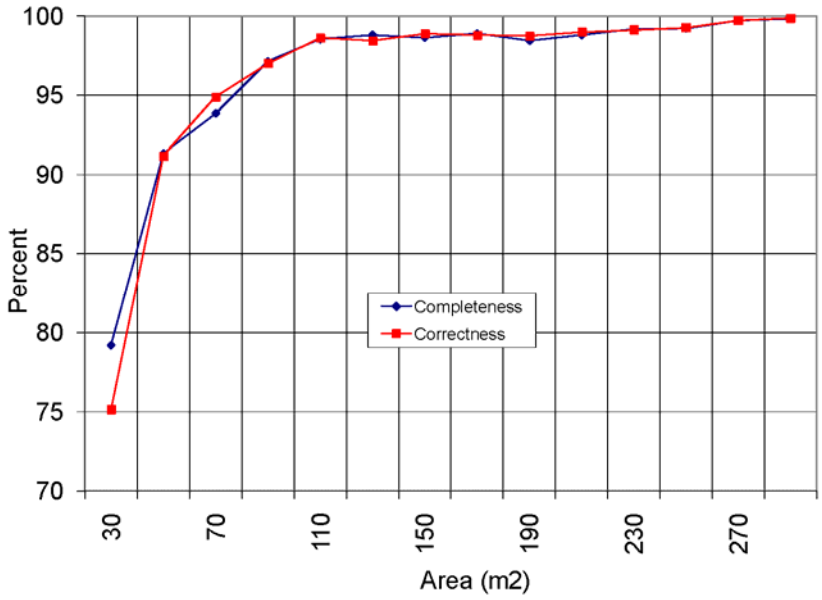

Figure 5: Completeness and correctness derived for the detection process plotted against size of detected areas.

5 CONCLUSION

In this paper, we have applied a powerful method to combine change detection techniques with different performance based on the simple majority vote. To test the algorithm, four change detection methods were based on LiDAR data of different two epochs. The results showed an improvement in terms of detection accuracy as well as omission and commission errors. Detection accuracies of individual algorithms were 84.7%, 88.3%, 90.2% and 91.6% for post-classification, image differencing, PCA and MNF respectively, whereas the proposed fusion algorithm gave an accuracy of 97.2% which is an improvement of around 5.6%. On the other hand, the proposed method showed a high level of automation in change detection process. These results demonstrate the overall advantages of the proposed algorithm for change detection that could be applicable for detecting changes in buildings damaged in a disaster such as an earthquake.If two LiDAR flights could be carried out before and after an earthquake, the change detection results can reveal the collapsed buildings. Although this paper used only heights of buildings for change detection, it is well-prepared and opened to integrate elevation and intensity distribution in future studies. Spectral information from aerial imagery can also be applied along with LiDAR data in order to improve the performance of the proposed method, and to refine the results.

REFERENCES

Armenakis C., F. Leduc, I. Cyr, F. Savopol, F. Cavayas (2003). A comparative analysis of scanned maps and imagery for mapping applications. *ISPRS Journal of Photogrammetry and Remote Sensing*, 57:304–14.

Baltsavias E. (1999). Airborne laser scanning: basic relations and formulas. *ISPRS Journal of Photogrammetry and Remote Sensing*, 54(2-3), pp. 199-214.

Brzank A., Heipke C., Goepfert J. (2009). Morphologic Change Detection in the Wadden Sea from LiDAR Data. *ISPRS Congress*, Volume XXXVII, Part B8, Commission VIII, ISSN 1682-1750, 3 to 11 July 2008, Beijing, China, p.647 ff.

Chen L. C. (2010). Detection of building changes from aerial images and light detection and ranging (LIDAR) data. *Journal of Applied Remote Sensing*, Vol. 4, 041870 (19 November 2010).

Clifton C. (2003). Change Detection in Overhead Imagery using Neural Networks. *International Journal of Applied Intelligence*, 18(2):215-234.

Collins J. B., C. E. Woodcock (1994). Change detection using the Gramm-Schmidt transformation applied to mapping forest mortality. *Remote Sensing of Environment*, 50:267–79.

Congalton R.G. (1991). A review of assessing the accuracy of classifications of remotely sensed data. *Remote Sensing of Environment*, 37(1):35–46.

Girardeau-Montaut D., Roux M., Marc R., Thibault G. (2005). Change Detection on Points Cloud Data Acquired with a Ground Laser Scanner, *International Archives of Photogrammetry, Remote Sensing and Spatial Information Sciences*, XXXVI (Pt. 3/W19):30-35.

Green A. A., Berman M., Switzer P., Craig M. D. (1988). A transformation for ordering multispectral data in terms of image quality with implications for noise removal: *IEEE Transactions on Geoscience and Remote Sensing*, v. 26, no. 1, p. 65-74.

Hashimoto S., Tadono T., Onosatoa M., Horib M. and Moriyamab T. (2011). An Approach for Automatic Change Inference in High Resolution Satellite Images. *34th International Symposium on Remote Sensing of Environment*, The GEOSS Era: Towards Operational Environmental Monitoring, Sydney, Australia, 10-15 April 2011.

Heipke C., Mayer H., Wiedemann C., Jamet O. (1997). Evaluation of automatic road extraction. *International Archives of Photogrammetry and Remote Sensing*, XXXII-2-3W3, Haifa, Israel, pp. 47–56.

Huang C., Chen L. (2007). Detection of Building Changes from LiDAR Data and Aerial Imagery. In: *ACRS 2007: proceedings of the 28th Asian conference on remote sensing*, 12-16 November 2007, Kuala Lumpur, Malaysia.

Jung F. (2004). Detecting Building Changes from Multitemporal Aerial Stereopairs. ISPRS *Journal of Photogrammetry and Remote Sensing*, 58:187-201.

Kumar A. (2011). Temporal Changes in Mangrove Cover Between 1972 and 2001 Along the South Coast of the Arabian Gulf. *34th International Symposium on Remote Sensing of Environment*, The GEOSS Era: Towards Operational Environmental Monitoring, Sydney, Australia, 10-15 April 2011.

Knudsen T., Olsen B. P. (2003). Automated Change Detection for Updates of Digital Map Databases, *Photogrammetric Engineering and Remote Sensing*, vol. 69 (11), pp. 1289-1297, 2003.

Legendre P., L. Legendre (1998). *Numerical Ecology*. Elsevier Science, Amsterdam. 853 p.

Matikainen L., Hyyppä J., Hyyppä H. (2004). Automatic Detection of Changes from Laser Scanner and Aerial Image Data for Updating Building Maps. *International Archives of Photogrammetry, Remote sensing and Spatial Information Sciences*, XXXV (B2):434-439.

Murakami H., Nakagawa K., Hasegawa H. Shibata T. (1999). Change Detection of Buildings Using an Airborne Laser Scanner, *ISPRS Journal of Photogrammetry and Remote Sensing*, 54:148-152.

Niederöst M. (2001). Automated update of building information in maps using medium-scale imagery (1:15,000), Automatic Extraction of Man-Made Objects from Aerial and Space Images (III), Baltsavias, E., Gruen, A., Van Gool, L. (Eds.), Balkema, Lisse, pp. 161-170.

Nielsen A. A., Canty M. J. (2011). A Method for Unsupervised Change Detection and Automatic Radiometric Normalization in Multispectral Data. *34th International Symposium on Remote*

Sensing of Environment, The GEOSS Era: Towards Operational Environmental Monitoring, Sydney, Australia, 10-15 April 2011.

Rottensteiner F., Trinder J., Clode S. and Kubik K. (2007). Building detection by fusion of airborne laser scanner data and multi-spectral images: Performance Evaluation and Sensitivity Analysis, *ISPRS Journal of Photogrammetry & Remote Sensing*, 62, pp. 135–149.

Spitzer H., R. Franck, M. Kollewe, N. Rega, A. Rothkirch, R. Wiemker (2001). Change Detection with 1 m Resolution Satellite and Aerial Images. In: *Proceedings of the IEEE 2001 International Geoscience and Remote Sensing Symposium*. Vol. 5, pp. 2256-2258.

Clifton C. (2003). Change Detection in Overhead Imagery using Neural Networks. *International Journal of Applied Intelligence*, 18(2):215-234.

Tuong T.V., Matsuoka M., Yamazaki F. (2004). LIDAR-based Change Detection of Buildings in Dense Urban Areas, *Proceedings of the IEEE International Geoscience and Remote Sensing Symposium*, Vol. 5, pp.3413-3416.

Vapnik V. (1979). *Estimation of Dependences Based on Empirical Data [in Russian]*. Nauka, Moscow, 1979. (English translation: Springer Verlag, New York, 1982).

Walter V. (2004a). Object-based classification of remote sensing data for change detection, *ISPRS Journal of Photogrammetry & Remote Sensing*, vol. 58, pp. 225– 238, 2004.

Walter V. (2004b). Object-based Evaluation of LiDAR and Multispectral Data for Automatic Change Detection in GIS Databases, *IAPRS*, 35(B2):723-728.

Waske B. (2007). Classifying multisensor remote sensing data: concepts, algorithms and applications. *PhD thesis, Bonn University, Germany*.

ACKNOWLEDGEMENTS

The authors would like to acknowledge Asia Air Survey Co. Ltd for the provision of the LiDAR datasets.